

SCIENTIFIC REPORTS

OPEN

Selective Inactivation of Intracellular BiP/GRP78 Attenuates Endothelial Inflammation and Permeability in Acute Lung Injury

Antony Leonard¹, Valerie Grose¹, Adrienne W. Paton², James C. Paton², David I. Yule³, Arshad Rahman¹ & Fabeha Fazal¹

The role of Endoplasmic Reticulum Chaperone and Signaling Regulator BiP/GRP78 in acute inflammatory injury, particularly in the context of lung endothelium, is poorly defined. In his study, we monitored the effect of SubAB, a holoenzyme that cleaves and specifically inactivates BiP/GRP78 and its inactive mutant SubA_{A272}B on lung inflammatory injury in an aerosolized LPS inhalation mouse model of acute lung injury (ALI). Analysis of lung homogenates and bronchoalveolar lavage (BAL) fluid showed that LPS-induced lung inflammation and injury were significantly inhibited in SubAB- but not in SubA_{A272}B-treated mice. SubAB-treated mice were also protected from LPS-induced decrease in lung compliance. Gene transfer of dominant negative mutant of BiP in the lung endothelium protected against LPS-induced lung inflammatory responses. Consistent with this, stimulation of endothelial cells (EC) with thrombin caused an increase in BiP/GRP78 levels and inhibition of ER stress with 4-phenylbutyric acid (4-PBA) prevented this response as well as increase in VCAM-1, ICAM-1, IL-6, and IL-8 levels. Importantly, thrombin-induced Ca²⁺ signaling and EC permeability were also prevented upon BiP/GRP78 inactivation. The above EC responses are mediated by intracellular BiP/GRP78 and not by cell surface BiP/GRP78. Together, these data identify intracellular BiP/GRP78 as a novel regulator of endothelial dysfunction associated with ALI.

Acute lung injury (ALI) is a common cause of respiratory failure in critically ill patients with a mortality rate of 38.5%¹. ALI can be precipitated by either direct insults such as pneumonia, aspiration or via indirect insults such as sepsis and multiple trauma, to the lungs². The vascular endothelium forming the innermost lining of all pulmonary blood vessels is the major barrier that protects air spaces against vascular fluid entry. Upon microbial infection, products such as lipopolysaccharides (LPS) from Gram-negative bacteria are released into the pulmonary circulation where they interact with lung vascular endothelial cells (EC) lining the blood capillaries. Vascular EC exposed to bacterial toxins secrete inflammatory and chemotactic substances, express adhesion molecules and demonstrate loss of barrier integrity¹. Disruption of pulmonary endothelial barrier function and acquisition of a proinflammatory phenotype are among the major pathogenic features of ALI^{3,4}.

Activation of the transcription factor NF- κ B is a key mechanism responsible for the acquisition of the proinflammatory phenotype in the lung. Activated NF- κ B converts the otherwise “antiadhesive” lung vascular endothelium into a “proadhesive” one via activation of adhesion molecules (ICAM-1, VCAM-1), cytokines (TNF-, IL1 β , IL-6), and chemokines (IL-8 and MCP-1), which in turn facilitates the adhesion and subsequent transendothelial migration of inflammatory cells, particularly neutrophils (polymorphonuclear leukocytes [PMN]) into the alveolar air space^{5–10}. The mechanism underlying increased lung endothelial permeability involves disruption of VE-cadherin homodimers, the key components of adherens junction (AJs). In addition to VE-cadherin disassembly, actin-myosin interaction is critical to EC barrier disruption caused by proinflammatory agonists^{11–15}. Together, these events (NF- κ B activation and VE-cadherin disassembly) contribute to ALI pathogenesis^{16–20}.

¹Department of Pediatrics, Lung Biology and Disease Program, University of Rochester School of Medicine and Dentistry, Rochester, New York, 14642, USA. ²Research Centre for Infectious Diseases, Department of Molecular and Biomedical Science, University of Adelaide, Adelaide, South Australia, Australia. ³Department of Pharmacology & Physiology, University of Rochester School of Medicine and Dentistry, Rochester, New York, 14642, USA. Correspondence and requests for materials should be addressed to F.F. (email: Fabeha_Fazal@URMC.Rochester.edu)

The endoplasmic reticulum (ER) is a major site for the synthesis and maturation of secretory and membrane proteins and therefore plays essential roles in physiological regulation of many cellular processes²¹. BiP/GRP78 (Binding Immunoglobulin Protein/78-kDa glucose-regulated protein), also referred to as heat-shock protein A5 (HSPA5), is primarily regarded as an ER chaperone involved in protein folding and assembly, Ca²⁺ homeostasis, and regulating ER stress signaling. Disturbances in ER homeostasis, due to glucose deprivation, disturbances in Ca²⁺ homeostasis, viral and bacterial infections, can cause imbalance in the luminal flux of the newly synthesized unfolded or misfolded peptides resulting in a condition known as ER stress²². To combat ER stress an adaptive mechanism called the unfolded protein response (UPR) is activated. One of the pathways activated under UPR involves expression of ER chaperone BiP/GRP78 to assist in proper protein folding, maintain chaperone homeostasis, and support cell survival. However, recent studies have shown that BiP/GRP78 not only resides in the ER lumen, but also outside the ER (cytoplasm, mitochondria, nucleus, and plasma membrane), and performs different functions in different cellular compartments²³. Intracellular BiP/GRP78 regulates ER stress-induced signaling and apoptosis, whereas cell surface BiP/GRP78 acts as receptor for both viral entry and for proliferation and apoptotic signaling. Studies have shown that BiP/GRP78 is also critical to embryonic development, aging, insulin-mediated signaling and pathological conditions, including cancer, diabetes, obesity and neurological disorders^{24–27}. However, the role of BiP/GRP78 in *acute* inflammatory injury, particularly in the context of lung endothelium, remains largely unknown. In order to ascertain the role of BiP both in primary endothelial cells and in a LPS inhalation murine model of ALI, we used Subtilase cytotoxin (SubAB), the prototype of a family of AB5 cytotoxins produced by Shiga toxinogenic *Escherichia coli*, or its isolated catalytic A subunit (SubA), that specifically cleaves BiP/GRP78 between a dileucine motif (Leucine_{416/417}), resulting in inactivation of BiP^{28,29}. Our study identifies intracellular BiP/GRP78 as an important mediator of lung vascular inflammation and injury through its ability, at least in part, to activate EC inflammation and barrier disruption.

Results

BiP/GRP78 is a critical mediator of lung inflammation and injury.

In order to test the possibility whether BiP/GRP78 is a critical player in mediating lung vascular inflammation and injury we first determined if BiP expression was regulated in an aerosolized bacterial LPS inhalation mouse model of ALI. A marked increase in BiP/GRP78 expression was observed in lung homogenates of mice treated with LPS (Fig. 1A). No mortality was observed in these mice as they were exposed to a sublethal dose of LPS (0.5 mg/ml; 6 ml). Furthermore mice were treated intraperitoneally (i.p.) with BiP/GRP78 inhibitor SubAB or its inactive mutant SubA_{A272}B for 6 h and then challenged with LPS for 16 h. Analysis of lung homogenates from these mice showed that LPS inhalation induced the levels of proinflammatory mediators VCAM-1 and IL-1 β ; but these responses were strongly inhibited in SubAB treated mice (Fig. 1B,C). In contrast, mice pretreated with SubA_{A272}B showed no protection against LPS-induced increase in VCAM-1 and IL-1 β levels. Consistent with this, infiltration of neutrophils in the lung, as measured by myeloperoxidase (MPO) activity, was also inhibited in mice treated with SubAB but not in the mice treated with SubA_{A272}B (Fig. 1D). Analysis of the bronchoalveolar lavage (BAL) showed that LPS substantially induced albumin levels, an indicator of microvascular leakage; this response was inhibited by SubAB but not by SubA_{A272}B (Fig. 1E). We next determined the effect of SubAB and SubA_{A272}B on lung wet-to-dry weight ratio, an important indicator of lung tissue edema, and found that LPS-induced lung tissue edema was protected in the presence of SubAB (Fig. 1F). These data led us to determine if SubAB is also effective in improving lung function in mice challenged with LPS. To this end, we assessed the dynamic lung compliance in live ventilated mice and found that LPS-induced decrease in lung compliance was protected in mice pretreated with SubAB but not in mice pretreated with SubA_{A272}B (Fig. 1G). These data establish that BiP/GRP78 as a critical determinant of lung inflammatory injury in mice.

Endothelial BiP/GRP78 contributes to lung vascular inflammation.

In order to understand the role of endothelial BiP/GRP78 in LPS induced lung vascular inflammation, wild type C57BL/6 L mice were transduced with a plasmid expressing a dominant negative mutant of BiP/GRP78 (p-BiP/GRP78-DN) or empty vector (EV) via intravenous injection of cationic liposomes, which primarily targets the lung endothelium for gene transfer^{30–32}. Seventy-two hours after the injection, mice were challenged with LPS for 16 h. Lung homogenates were analyzed for expression of the transduced plasmid (p-BiP/GRP78-DN). Increased expression of BiP/GRP78 was observed in mice transduced with p-BiP/GRP78-DN compared to mice transduced with EV (Fig. 2A). Furthermore, BAL fluid was analyzed for the levels of proinflammatory mediators such as ICAM-1 and MCP-1 and for PMN recruitment. Data showed that LPS-induced ICAM-1 and MCP-1 levels as well as PMN infiltration were significantly inhibited in mice expressing BiP/GRP78-DN compared to mice transduced with EV (Fig. 2B–D). Together, these results indicate that endothelial BiP/GRP78 plays a vital role in causing lung vascular inflammation.

ER stress is critical to EC inflammation.

Because BiP/GRP78 is a known mediator of ER stress, we investigated if the ER stress-BiP/GRP78 axis is critical to EC inflammation associated with ALI. We determined if thrombin promotes BiP/GRP78 expression in an ER stress-dependent manner in EC. Stimulation of human pulmonary artery endothelial cells (HPAEC) with thrombin caused an increase in BiP/GRP78 levels and pretreatment of cells with the ER stress inhibitor 4-phenylbutyric acid (4-PBA)³³ prevented thrombin-induced increase in BiP/GRP78 level (Fig. 3A). We next determined whether the ER stress-BiP/GRP78 axis also mediates thrombin-induced EC inflammation. Results showed that pretreatment of cells with 4-PBA prevented thrombin-induced transcriptional activity of NF- κ B (Fig. 3B). Furthermore, a marked reduction in thrombin-induced ICAM-1, VCAM-1, IL-6 and IL-8 levels was noted in the presence of 4-PBA, consistent with its effect on NF- κ B activity (Fig. 3C–F). It should be noted that siRNA-mediated knockdown of BiP/GRP78 produced a similar effect on thrombin-induced EC inflammation²². Together, these data support a role for ER stress-BiP/GRP78 axis in EC inflammation.

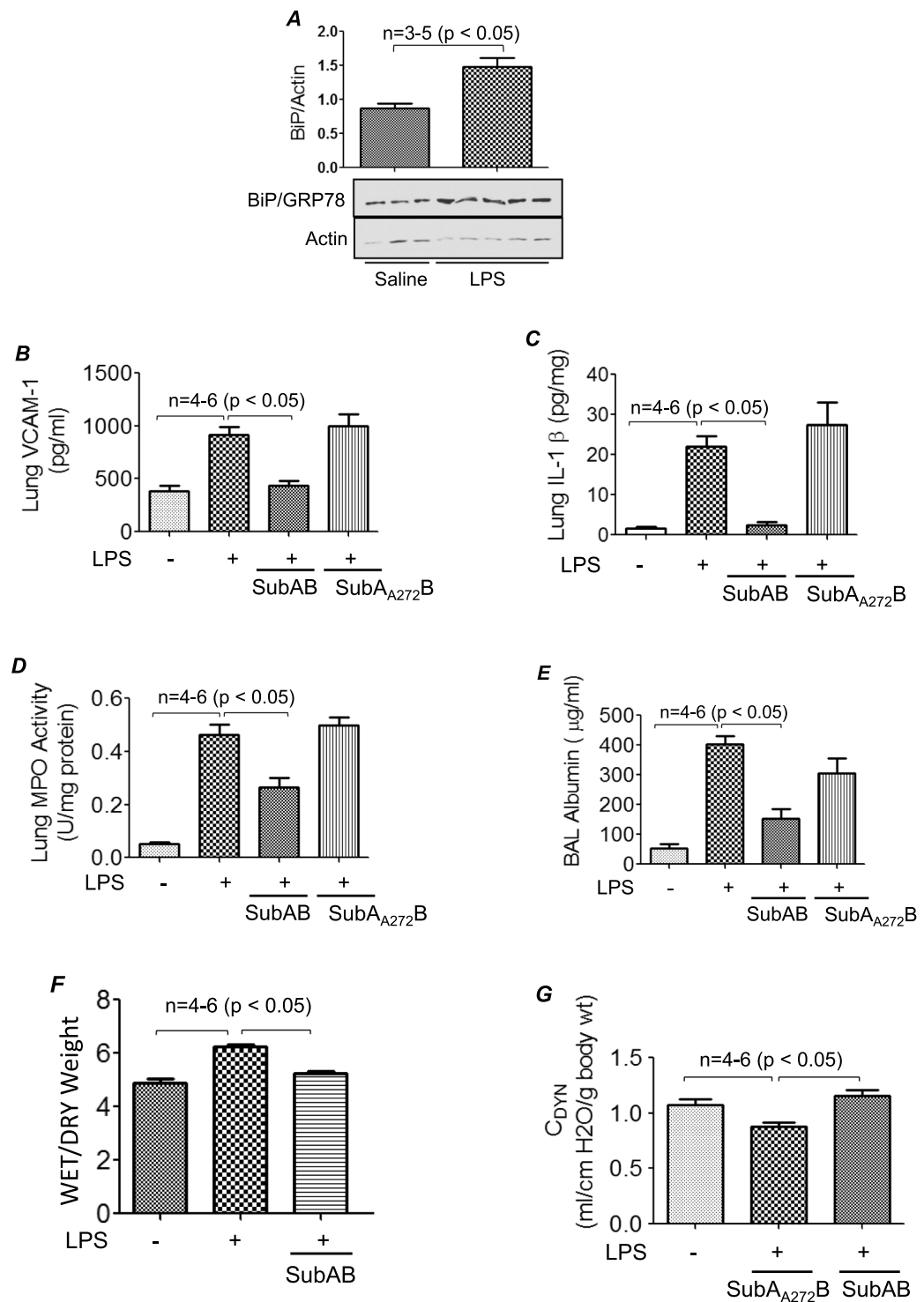


Figure 1. SubAB protects against LPS-induced lung inflammation and injury. Wild type C57BL/6 mice were injected i.p. with SubAB or mutant SubA_{A272}B (0.04 mg/kg bodyweight) for 6 h. Mice were then aerosolized with 6 ml of saline alone or saline containing *E. Coli* LPS (0.5 mg/ml) for 30 min. Eighteen hours after LPS challenge, lung homogenates were analyzed for levels of BiP/GRP78 (A), proinflammatory mediators VCAM-1 (B) and IL-1β (C) by ELISA and neutrophil sequestration by measuring tissue MPO activity (D). Bronchoalveolar lavage (BAL) fluids were analyzed for albumin levels (E) Lungs were analyzed for wet-to-dry weight ratio (F). Live ventilated mice were evaluated for dynamic lung compliance (G) using whole-body plethysmograph as described in Materials and Methods section.

Intracellular pool of BiP/GRP78 is critical for EC inflammation. BiP/GRP78 is shown to be present not only in the ER but in extra-ER regions as well, such as the cytosol and plasma membrane²³. In order to ascertain the role of intracellular versus cell surface BiP/GRP78 we used two specific inhibitors; SubAB and SubA.

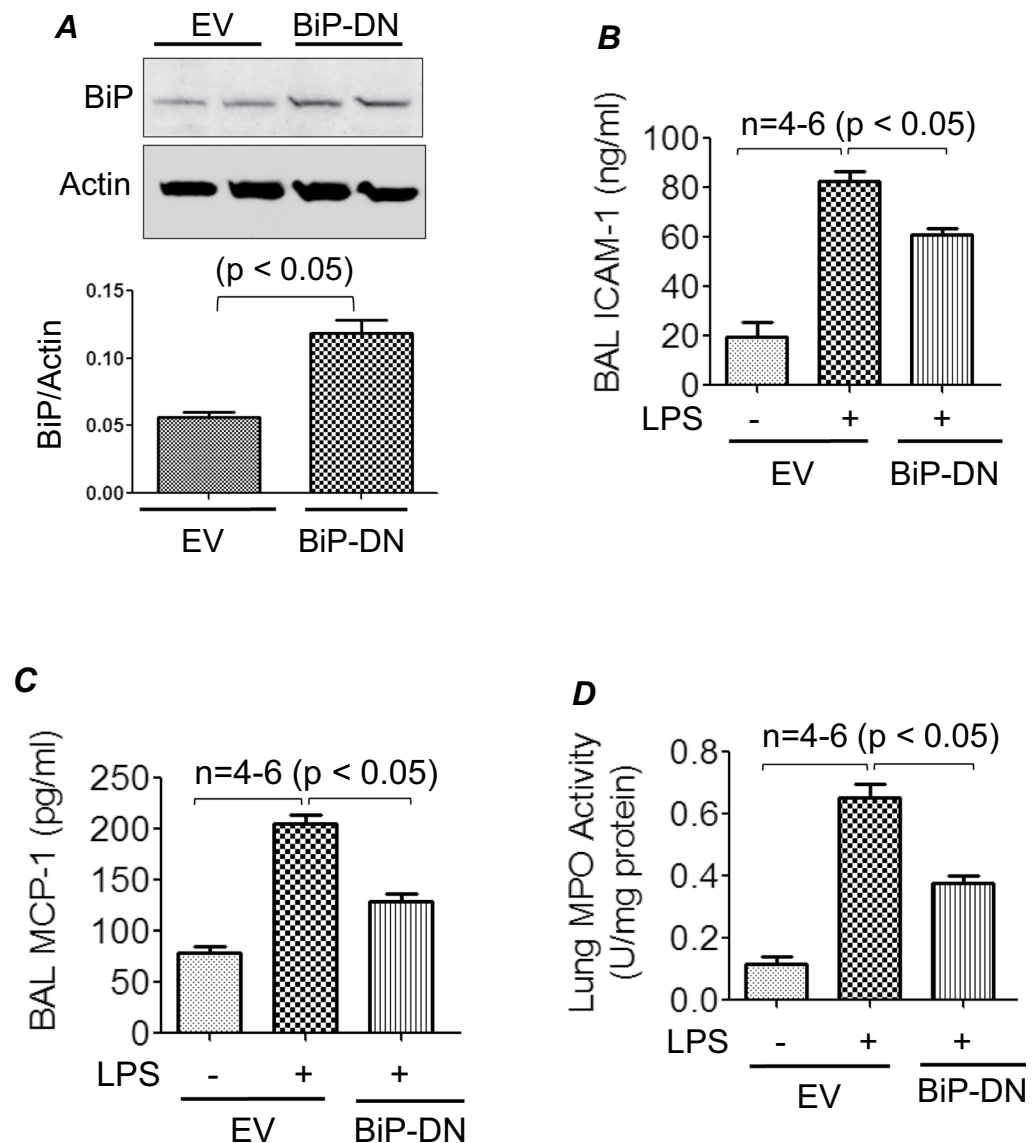


Figure 2. Cationic liposome mediated gene transfer of BiP/GRP78-DN dampens LPS-induced lung injury. WT C57BL/6 mice were injected i.v. with empty vector (EV)/liposome or dominant negative mutant BiP/GRP78 (BiP/GRP78-DN)/liposome complex. After 72 h, mice were aerosolized with 6 ml of saline alone or saline containing *E. Coli* LPS (0.5 mg/ml) for 30 min. Sixteen hours later, lung homogenates were analyzed for expression of BiP/GRP78-DN (A). BAL fluids were analyzed for ICAM-1 (B) and MCP-1 (C) levels. Lung homogenates were analyzed for MPO activity (D).

SubAB is a serine protease composed of a 35-kDa catalytic A subunit (SubA), and five 13-kDa B subunits. The A subunit contains the catalytic triad Asp₂₇₀, His₂₇₁ and Ser₂₇₂, which is responsible for cleaving BiP/GRP78 between Leucine₄₁₆₋₄₁₇ and thereby inhibiting its function. Mutation of Ser₂₇₂ to Ala₂₇₂ results in a catalytically inactive enzyme (SubA_{A272}B). The B subunit mediates binding to glycan receptors on the cell surface and is necessary for internalization and subsequent trafficking of the holoenzyme to the ER. Consequently, SubAB cleaves and inactivates the global pool of BiP/GRP78 (intracellular and cell surface), while SubA only cleaves and inactivates the cell surface BiP/GRP78^{28,29}. Importantly, both SubAB and SubA display extreme substrate specificity towards BiP/GRP78^{28,29}. Since not every cell type expresses BiP/GRP78 on the cell surface we first wanted to confirm the expression of cell surface BiP/GRP78 in HPAEC. Our data showed that BiP/GRP78 is expressed on endothelial cell surface in low levels and the majority of it resides intracellularly. Next, we confirmed the mode of action of SubAB and SubA towards BiP/GRP78 by western blot analysis (Fig. 4B). As expected, time course analysis showed that pretreatment of EC with SubA resulted in the appearance of cleaved BiP/GRP78 band (~28 kDa) only in cell culture supernatants and not in cell lysates, whereas pretreatment with SubAB generated the 28 kDa cleaved BiP/GRP78 band both in cell culture lysates and supernatants (Fig. 4B). Next, the effect of SubA was analyzed on thrombin-induced EC inflammation. Interestingly, SubA failed to inhibit thrombin-induced activation of NF- κ B and expression of ICAM-1, IL-8 and IL-6 (Fig. 4C-F). This is in contrast to the effect of SubAB

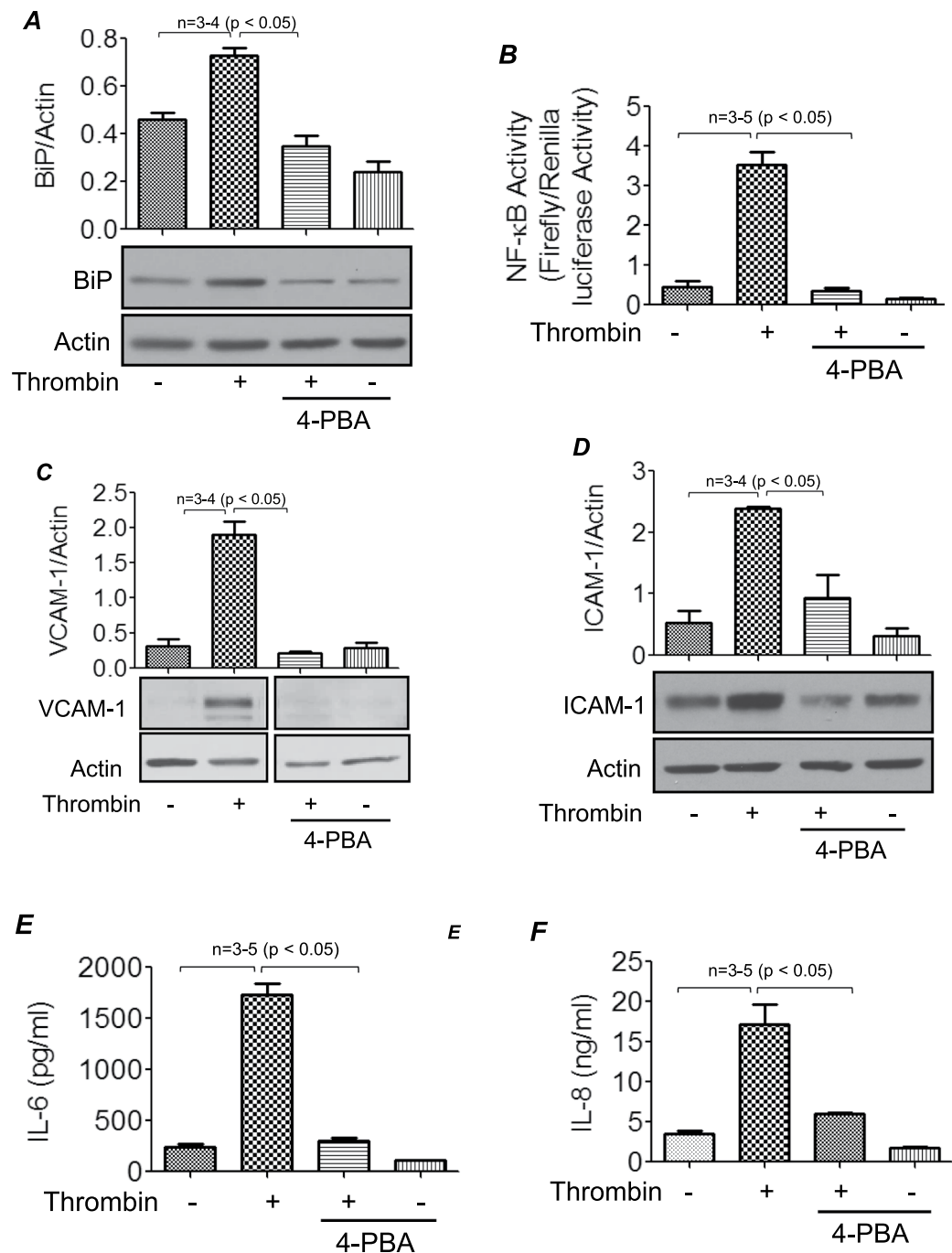


Figure 3. Thrombin-induced inflammatory responses are mitigated in the presence of ER stress inhibitor 4-PBA. HPAEC were pretreated with 4-PBA (10 mM) for 1 h followed by treatment with 5 U/ml thrombin for 6 h. Total cell lysates were probed for BiP/GRP78 (A). HPAEC were transfected with NF- κ B-LUC and pTKRLUC constructs by DEAE-dextran as described in Methods. Cells were then treated with 4-PBA (1 h) followed by thrombin treatment (5U/ml) for 6 h and cell extracts were prepared and assayed for Firefly and Renilla luciferase activities (B). Total cell lysates treated with 4-PBA followed by thrombin treatment were also probed for VCAM-1(C) and ICAM-1(D) by western blotting and cell supernatants were analyzed for IL-6 (E) and IL-8 (F) levels by ELISA. The blot in 3 C is cropped from two different parts of the same gel, as shown by white space.

which inhibits thrombin-induced EC inflammation (Fig. 4G)²². These data identify intracellular BiP/GRP78 as an important regulator of EC inflammation induced by thrombin.

BiP/GRP78 mediate EC adhesivity towards HL-60. In order to understand the functional relevance of BiP/GRP78 in EC inflammation, we assessed the adhesion of the neutrophilic cell line HL-60 to the activated EC (expressing adhesion molecules upon thrombin treatment)³⁴. Results showed that thrombin increased EC

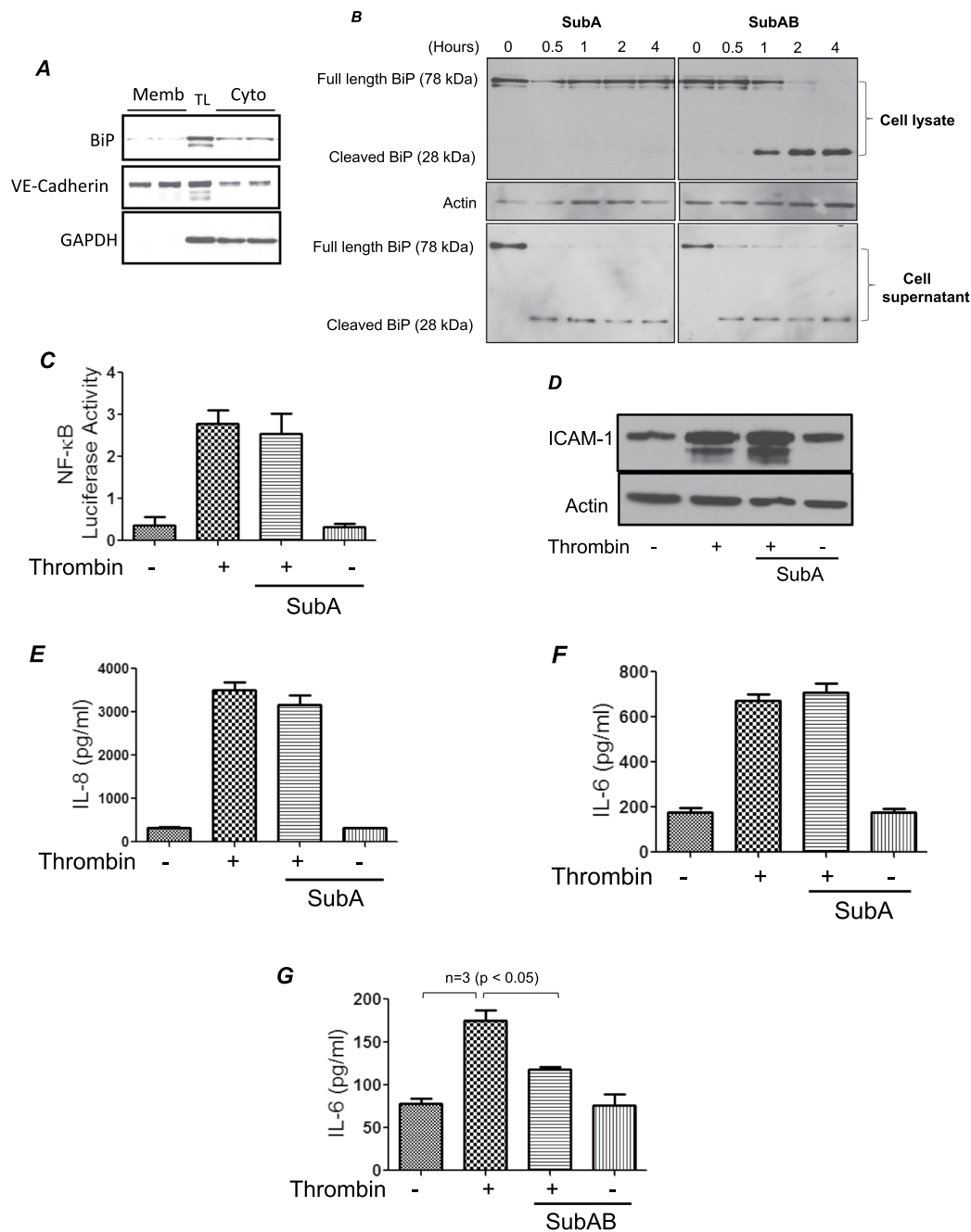


Figure 4. SubA fails to mediate thrombin-induced inflammatory response. Confluent HPAEC were biotinylated using Sulfo-NHS-SS-Biotin, subsequently lysed and labeled cell surface proteins were isolated using streptavidin beads and then separated on an SDS-PAGE and probed for BiP, VE-cadherin and GAPDH (A). TL is total lysate. HPAEC were treated with 0.1 $\mu\text{g/ml}$ of SubA and SubAB for the indicated time points. Cell lysates and corresponding cell supernatants were immunoblotted for BiP/GRP78 to monitor the cleavage of BiP/GRP78 by SubA and SubAB (B). The blot in 4B is cropped from two different parts of the same gel, as shown by white space. HPAEC were transfected with NF- κ BLUC and pTKRLUC constructs by DEAE-dextran as described in Materials and Methods section. Following transfection cells were treated with 0.1 $\mu\text{g/ml}$ of SubA for 3 h and then by 5 U/ml of thrombin for 6 h. Total cell lysates were prepared and assayed for Firefly and Renilla luciferase activities (C). Confluent HPAEC were pretreated with SubA for 3 h followed by thrombin treatment (5 U/ml) for 6 h. Cell lysates were probed for ICAM-1 (D) and cell supernatants were analyzed for IL-8 (E) and IL-6 (F) by ELISA. HPAEC were pretreated with SubAB for 3 h followed by thrombin treatment (5U/ml) for 6 h. Total cell lysates were probed for IL-6 (G) by ELISA.

adhesivity toward HL-60 cells and that SubAB prevented this response. Unlike SubAB, SubA_{A272}B showed no significant effect on thrombin-induced EC adhesivity toward HL-60 cells (Fig. 5). In contrast, SubA failed to inhibit adhesion of HL60 cells to EC stimulated with thrombin (Fig. 5). These data are consistent with the effects

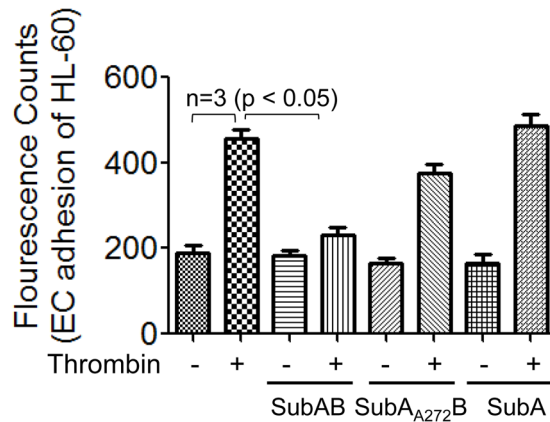


Figure 5. SubAB selectively inhibits adhesion of HL-60 to thrombin activated EC. HPAEC were grown to confluence in 96-well black polystyrene plates. Confluent monolayers were treated with 0.1 $\mu\text{g/ml}$ of SubAB, SubA_{A272}B or SubA followed by treatment with thrombin (5 U/ml) for 5 h. HL-60 cells were labelled with 2.5 μM Calcein-AM for 30 min. Calcein-AM labeled HL-60 cells were added to each well for 1 h at 37 °C followed by gentle wash with Phenol Red free DMEM media 4 times. Fluorescence was measured using a fluorescent plate reader at an excitation of 495 nm.

of SubAB, SubA_{A272}B²² and SubA on thrombin-induced expression of proinflammatory genes (Fig. 4D–F) and support a role of intracellular BiP/GRP78 in regulating thrombin-induced EC adhesion.

BiP/GRP78 is critical to thrombin-induced EC permeability via VE-cadherin disassembly.

Because loss of endothelial barrier integrity is another major pathogenic feature of ALI, we next addressed the role of BiP/GRP78 in thrombin-induced EC permeability. Trans-endothelial resistance (TER), which is a real time measurement of EC permeability, was performed after thrombin challenge³⁵. Maximal decrease in TER was observed around 0.5 h and the cells gradually recovered to baseline by 2–4 h. Inactivation of BiP/GRP78 by SubAB not only protected against thrombin-induced decrease in TER at earlier time points (0.25–1 h) but also enhanced the recovery after 2.5 h (Fig. 6A). In contrast, SubA_{A272}B not only failed to protect against thrombin-induced decrease in TER but also slowed the recovery after 1 h of thrombin challenge (Fig. 6A). These data are consistent with the protective effect of BiP/GRP78 knockdown on thrombin-induced inter-endothelial gap formation²². Interestingly, however, unlike SubAB, SubA had no effect on thrombin-induced decrease in TER (Fig. 6B). Together these data indicate a role of intracellular BiP/GRP78 in mediating EC permeability. Next, we determined whether the protection by SubAB against thrombin-induced decrease in TER is mediated via loss of VE-cadherin at AJs. Confocal microscopy revealed that thrombin-induced a decrease in immunostaining of VE-cadherin at AJs, whereas pretreatment with SubAB prevented the response (Fig. 6C). These data identify intracellular BiP/GRP78 as a critical mediator of EC barrier disruption through its ability to induce VE-cadherin disassembly.

BiP/GRP78 is critical to thrombin-induced Ca²⁺ signaling in EC. In order to further explore the mechanism of thrombin-induced EC permeability, we determined the role of BiP/GRP78 in mediating Ca²⁺ signaling, a critical determinant of EC permeability¹⁴. HPAEC were pretreated with SubAB, SubA or its inactive mutant SubA_{A272}B and then loaded with Fura2-AM for 15 min. Ratiometric measurements of intracellular Ca²⁺ were made in response to thrombin during extracellular Ca²⁺ depletion-repletion conditions. Results indicate that while inactivation of BiP/GRP78 by SubAB completely blocked the store-operated Ca²⁺ entry from the extracellular medium (represented by 2nd peak), it only partially inhibited Ca²⁺ release from the ER stores (indicated by the first peak) (Fig. 7A,B). In contrast, cells treated with SubA and SubA_{A272}B showed no effect on both Ca²⁺ release and entry (Fig. 7A,B). In a related experiment, we also assessed the effect of SubAB on cyclopiazonic acid (CPA)-induced Ca²⁺ signaling. It should be noted that CPA, like thapsigargin, induces store depletion-mediated Ca²⁺ entry via inhibition of sarcoendoplasmic reticulum Ca²⁺ATPase (SERCA)³⁶. We found that SubAB abolished store-operated Ca²⁺ entry but had no effect on Ca²⁺ release response caused by CPA (Fig. 7C,D). Together, these data indicate a novel role of BiP/GRP78 in the mechanism of store-operated Ca²⁺ entry.

Discussion

In the present study, we have uncovered BiP/GRP78 as a critical determinant of lung vascular inflammation and injury via its ability to mediate EC permeability and inflammation. Using an aerosolized bacterial LPS inhalation mouse model of ALI, we found that inactivating BiP/GRP78 using SubAB protected against LPS-induced lung inflammation and injury and LPS-induced decrease in lung compliance. Introduction of BiP/GRP78-DN via cationic liposomes, which specifically target the lung endothelium for gene transfer³², also dampened LPS-induced proinflammatory gene expression and lung PMN infiltration, indicating a critical role of endothelial BiP/GRP78 in the mechanism of lung vascular inflammation. *In vitro* studies, using cultured EC revealed that thrombin induced an increase in BiP/GRP78 levels and pretreatment of cells with ER stress inhibitor 4-PBA prevented this response. Consistent with a role of BiP in EC inflammation²², 4-PBA also inhibited thrombin-induced activation of NF- κ B and expression of proinflammatory genes, implicating a role of ER stress-BiP/GRP78 axis in EC

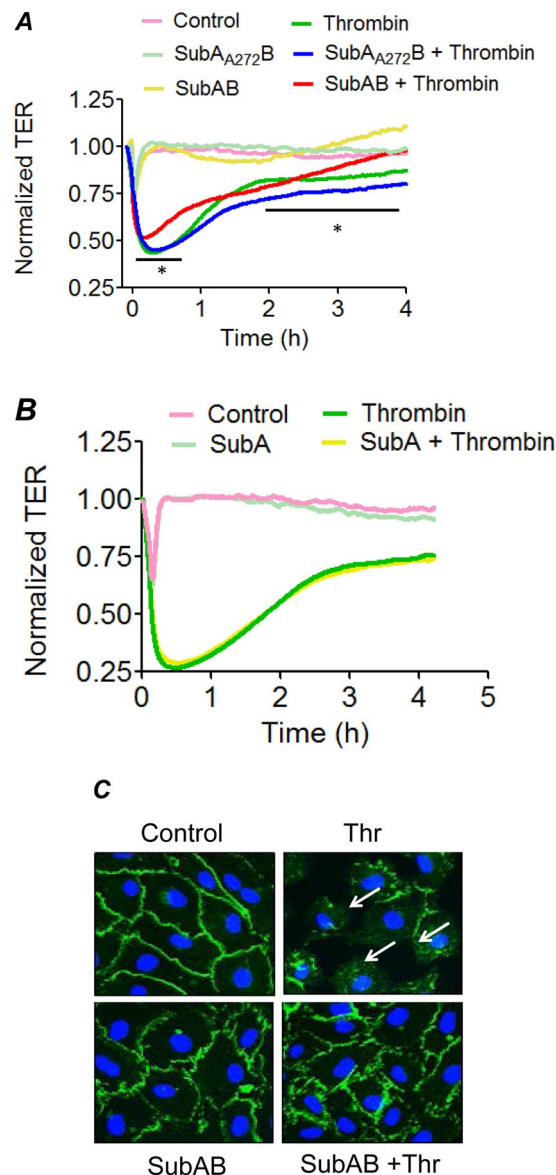


Figure 6. SubAB protects against thrombin-induced endothelial barrier disruption and VE-Cadherin disassembly. Confluent HPAEC grown on gold electrode plates were treated with 0.1 $\mu\text{g}/\text{ml}$ of SubAB or SubA_{A272}B (A) or SubA (B) for 3 h and then challenged with thrombin (2.5 U/ml). Real time changes in transendothelial electrical resistance (TER) were measured to monitor endothelial barrier function after thrombin treatment (A,B). Data are mean \pm SE ($n = 3-5$ for each condition). *Difference between thrombin treated versus thrombin + SubAB treated ($p < 0.05$). HPAEC grown to confluence on 2% gelatin coated coverslips were treated with 0.1 $\mu\text{g}/\text{ml}$ of SubAB for 3 h followed by treatment with thrombin (5 U/ml) for 15 min. Immunofluorescence was performed to visualize VE-cadherin (green) and nuclei (blue) (C). Arrows indicate disruption of VE-cadherin staining. Images are representative of 3 experiments.

inflammation. Our data also reveal a novel role of BiP/GRP78 in mediating EC permeability by virtue of activating Ca^{2+} signaling and promoting VE-cadherin disassembly. We further show that it is the intracellular BiP/GRP78 that mediates thrombin-induced EC inflammation and barrier disruption. Together, our data indicates that intracellular BiP/GRP78 contributes to ALI pathogenesis, at least in part, through its ability to induce inflammation and permeability in EC.

Alterations in pulmonary endothelium play a central role in the pathogenesis of several chronic and acute lung diseases. The main characteristics of pulmonary endothelial dysfunction are reflected by increased permeability leading to vascular leakage, edema formation, and acquisition of proinflammatory phenotype with increased expression of inflammatory mediators leading to PMN extravasation. In the present study, we analyzed the role of BiP/GRP78 in the pathogenesis of ALI in the context of pulmonary endothelium. Our results indicate that BiP/GRP78 contributes to lung vascular inflammation and injury. Intraperitoneal injections of BiP/GRP78 inhibitor SubAB decreased lung vascular injury caused by LPS. Moreover, pretreatment of mice with SubAB was associated

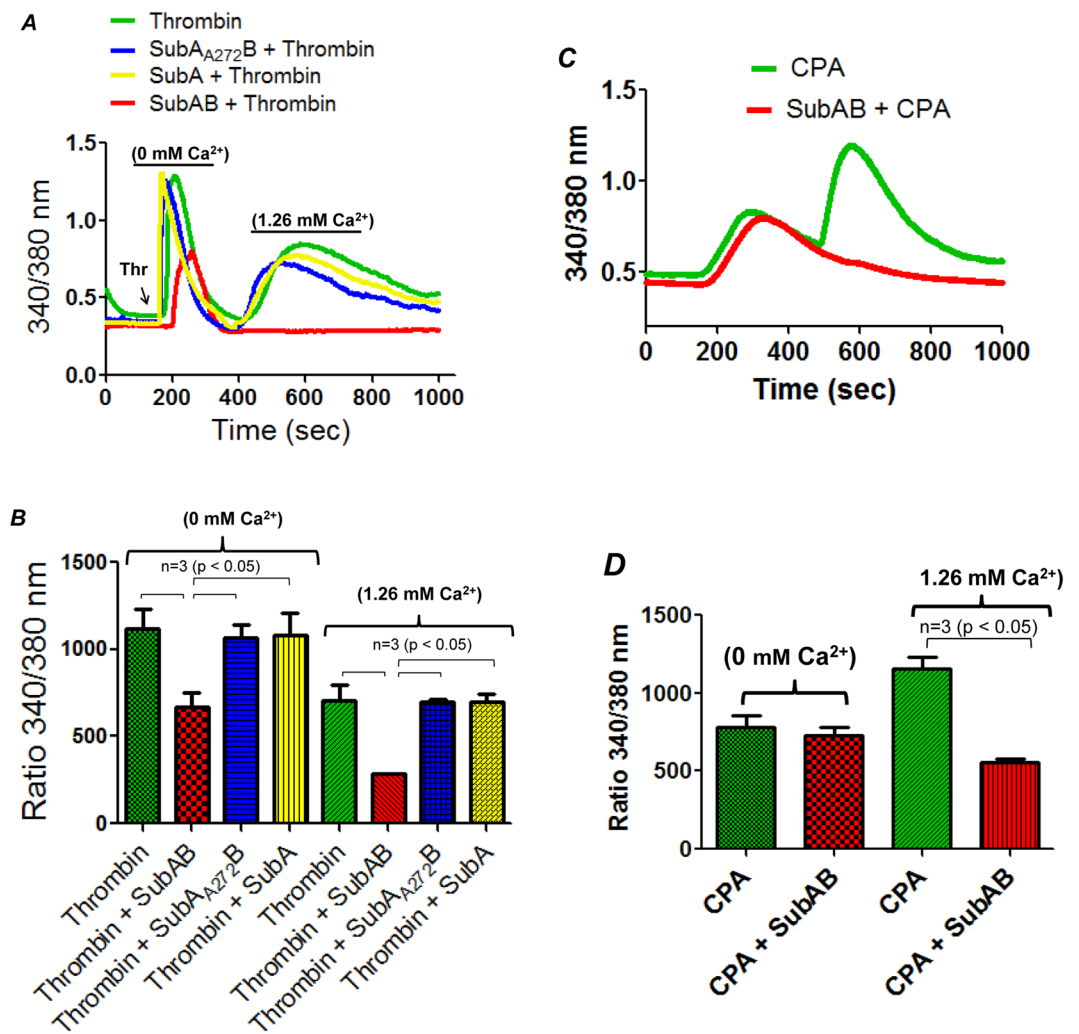


Figure 7. SubAB inhibits thrombin-induced Ca^{2+} release and entry in EC. HPAEC grown to confluence on 25 mm coverslips were treated with 0.1 $\mu\text{g}/\text{ml}$ of SubAB or SubA or its inactive mutant SubA_{A272}B for 3 h. Cells were then loaded with Fura2-AM for 30 min and washed twice with Ca^{2+} free HBSS buffer and mounted on an inverted microscope. Calcium release from the intracellular stores was determined by perfusing Ca^{2+} free imaging buffer and stimulating cells with thrombin (2.5 U/ml). Store-operated Ca^{2+} entry was measured following addition of 1.26 mM Ca^{2+} (A,B). HPAEC treated with or without SubAB were loaded with Fura2-AM and stimulated with 30 μM CPA in the absence of extracellular Ca^{2+} , to deplete ER Ca^{2+} . This was followed by re-addition of 1.26 mM Ca^{2+} to determine Ca^{2+} entry (C,D). Fura-2 ratio (F-ratio 340/380) was calculated and analyzed with NIS-Element AR 3.0 Software. CPA, is cyclopiazonic acid.

with reduced lung PMN sequestration and migration caused by LPS. Consistent with this, LPS-induced levels of proinflammatory mediators such as adhesion molecules, cytokines, and chemokines, which are required for adhesion of PMN to the endothelium and subsequent extravasation of adherent PMN into the surrounding tissues, were reduced in the lungs of SubAB-treated mice compared to SubA_{A272}B-treated mice. Importantly, LPS-induced decrease in lung compliance was protected in mice treated with SubAB but not in mice treated with SubA_{A272}B. Our data highlight a novel role of BiP/GRP78 as a proinflammatory molecule in LPS-induced lung inflammation and injury.

Since BiP/GRP78 is an inherently prosurvival/antiapoptotic protein, it is expressed at high levels in the cytoplasm of cancer cells from where a small fraction of it translocates to the plasma membrane to serve as receptor, and is critical to tumor cell signaling and viability²³. Recent studies have identified BiP/GRP78 on the surface of endothelial cells as well^{37,38}. Hence, we analyzed the role of intracellular versus cell surface BiP/GRP78 in EC inflammation and barrier disruption using the holoenzyme SubAB and SubA. SubAB specifically cleaves and inactivates the global (intracellular and cell surface) pool of BiP/GRP78 whereas SubA cleaves only the cell surface BiP/GRP78²⁹, as it lacks the B subunit required for internalization of the holoenzyme. Our data indicate that unlike cancer cells, only a small fraction of BiP/GRP78 is expressed on EC cell surface and it's the intracellular BiP/GRP78 that mediates thrombin-induced EC inflammation and permeability. Furthermore, we demonstrate that BiP/GRP78 inactivation by SubAB protected against thrombin-induced EC permeability by

initially decreasing the barrier disruption and later by increasing the barrier recovery. Mechanistically, we showed that BiP/GRP78 contributes to thrombin-induced EC permeability via VE-cadherin disassembly, a major mechanism of AJ disruptions and increased EC permeability^{14,39,40}.

Activation of Ca²⁺ signaling is critical for EC permeability and inflammation. Studies have shown that thrombin binding to protease activated receptor-1 (PAR1) activates heterotrimeric G proteins, G₁₂/G₁₃ and G_q thereby mediating generation of inositol 1,4,5-trisphosphate (IP₃), which in turn binds to inositol 1,4,5- trisphosphate receptor (IP₃R) on ER, and signals Ca²⁺ release from ER stores. Depletion of ER Ca²⁺ induces activation of store-operated channels (SOC) at the plasma membrane, resulting in Ca²⁺ entry and refilling of ER stores³⁶. Our data indicate that inactivation of BiP/GRP78 by SubAB abolished the store-depletion operated Ca²⁺ entry (SOCE) from the extracellular milieu but only partially inhibits the Ca²⁺ release in response to thrombin. SubAB also abolished the store-operated Ca²⁺ entry but had no effect on Ca²⁺ release response caused by CPA. Thus, these data identify a novel role of BiP/GRP78 in the mechanism of store-operated Ca²⁺ entry. Stromal interacting molecule 1 (STIM1), an ER Ca²⁺ sensor, is an important regulator of store-operated Ca²⁺ entry⁴¹. Upon sensing depletion of ER Ca²⁺, STIM1 organizes into a puncta and translocates to the close proximity of plasma membranes where it interacts with Ca²⁺-selective Orai1 channel to induce store-operated Ca²⁺ entry in EC^{42–45}. Given that both BiP/GRP78 and STIM1 are ER proteins, it is likely that BiP/GRP78 associates with STIM1 in the ER and that this interaction is vital for STIM1 function, and thereby store-operated Ca²⁺ entry; however, this possibility remains to be addressed.

Together, our data show that both EC inflammation and permeability are regulated by the intracellular BiP/GRP78 and not by cell surface BiP/GRP78. It should, however, be noted that other studies have shown that BiP/GRP78 functions as a cell surface receptor mediating barrier protective effects of oxidized phospholipids (OxPLs)³⁷. It is likely that stimulation of EC with barrier protective agents such as OxPAPC results in the activation of cell surface BiP/GRP78 which in turn activates the anti-inflammatory signaling cascade, whereas agents such as thrombin, which are potent inducers of EC permeability, engage the intracellular pool of BiP/GRP78 to induce proinflammatory phenotype in EC. In view of these findings highlighting a role of BiP/GRP78 in EC inflammation and permeability, we investigated the contribution of endothelial BiP/GRP78 in lung inflammatory responses. We found that expression of BiP/GRP78-DN in the lung endothelium was effective in reducing the expression of pro-inflammatory mediators and lung PMN infiltration in mice challenged with LPS. These data underscore the importance of endothelial BiP/GRP78 in lung inflammatory injury²². However, it should be stressed that these data do not exclude the involvement of BiP/GRP78 in alveolar epithelial cells and macrophages in this model of ALI. The effects of SubAB in reducing the levels of IL-1 β and MCP-1 that are also produced by epithelial and inflammatory cells besides EC support such a possibility. Thus, analyzing the specific contribution of BiP/GRP78 in endothelial vs. epithelial cells or macrophages in the context of ALI will require additional studies using mice with cell-specific deletion of BiP/GRP78.

Materials and Methods

Reagents. Human alpha thrombin was obtained from Enzyme Research Laboratories (South Bend, IN). Lipopolysaccharide (LPS) from *E. coli*, diethylaminoethyl (DEAE)-dextran, and 4-phenylbutyrate (4-PBA) were purchased from Sigma-Aldrich Chemical (St. Louis, MO). Polyclonal antibodies to VCAM-1, ICAM-1, I κ B α , RelA/p65, and β -actin were from Santa Cruz Biotechnology (CA). Antibodies to VE-cadherin were purchased from Abcam (Cambridge, MA) and BD Biosciences (San Jose, CA). BiP/GRP78 polyclonal antibody was obtained from Cell Signaling Technology (Beverly, MA). Expression vector encoding Wild type BiP/GRP78 and dominant negative BiP/GRP78 were from Addgene. SubAB, SubA and the non-active derivative SubA_{A272}B were purified as previously described^{28,29,46}. All other materials were from VWR Scientific Products Corporation (Gaithersburg, MD) and Fisher Scientific (Pittsburgh, PA).

Murine model of ALI. Male 8- to 10-wk-old wild-type (WT) C57BL/6 mice (Jackson, Bar Harbor, ME) were exposed to an aerosol of saline alone or saline containing *Escherichia coli* LPS (0.5 mg/ml, 6 ml) for 30 min in a chamber, as described⁴⁷. All animal care and treatment procedures were approved by the University of Rochester Committee on Animal Resources and performed in accordance with National Institutes of Health guidelines.

Measurement of lung inflammation and injury. Mouse lung homogenates were prepared in radioimmune precipitation (RIPA) buffer supplemented with protease inhibitor cocktail (Sigma-Aldrich) as described^{17,18,47}. The levels of ICAM-1, IL-1 β , albumin, and MCP-1 in BAL fluids were determined using ELISA kits from R&D Systems (Minneapolis, MN) as described^{17,18}. VCAM-1 levels in lung homogenates were determined by ELISA as described⁴⁷. The recruitment of PMN in the lung was determined by monitoring the myeloperoxidase activity in the lung tissues as described^{17,18}.

Wet-to-dry lung weight ratio was measured in mice that were not subjected to BAL⁴⁸. Blood was removed from the lungs by gentle infusion of 10 ml of phosphate-buffered saline containing 5 mM EDTA through the right ventricle. The lungs were excised en bloc and blotted dry, and the right lungs were snap-frozen in liquid nitrogen. The left lungs were weighed before and after being dried at 60 °C for 24 h to calculate lung wet-to-dry weight ratio⁴⁹.

Physiologic assessment of pulmonary function in live, ventilated mice. Dynamic lung compliance and lung resistance were measured in live ventilated mice using a whole-body plethysmograph (BUXCO Electronics, Wilmington, NC) connected to a Harvard rodent ventilator (Harvard Apparatus, South Natick, MA), as previously described⁵⁰. Dynamic lung compliance was normalized to the peak body weight of each animal. Respiratory rates were measured using whole-body unrestrained chambers (BUXCO Electronics). Data were collected and analyzed using the Biosystems XA software package (BUXCO Electronics).

Cationic liposome mediated gene transfer. Wild type C57BL/6L mice were injected i.v. with empty vector (EV)/liposome complex or dominant negative mutant BiP/GRP78 (pCMV-BiP/GRP78-DN)/liposome complex. After 72 hours mice were aerosolized with 6 ml of saline alone or saline containing *E. Coli* LPS (0.5 mg/ml) for 30 min. Sixteen hours later lung homogenates were analyzed for inflammation and injury^{32,47}.

Endothelial cells. Human pulmonary artery endothelial cells (HPAEC) were obtained from Lonza (Walkersville, MD) and cultured in 2% gelatin coated flasks using endothelial basal medium 2 (EBM2) with bullet kit additives (BioWhittaker, Walkersville, MD), as described^{47,51}. Experiments were performed in cells below *passage* 6.

Immunoblot analysis. After appropriate treatments HPAEC were lysed in radioimmune precipitation (RIPA) buffer. Total cell lysates were analyzed on SDS-PAGE followed by transfer on to nitrocellulose membranes. The membranes were subsequently incubated with primary antibody overnight at 4 °C followed by secondary antibody incubation at room temperature for 1 h. Subsequently the blot was developed using an enhanced chemiluminescence (ECL) method, as described¹⁸. Blots shown in the result section may have come from the membrane with more samples in various groups.

Reporter gene constructs and luciferase assay. The construct pNF- κ B-LUC containing five copies of consensus NF- κ B sequences linked to a minimal E1B promoter-luciferase gene was purchased from Stratagene (La Jolla, CA). Reporter gene transfections and luciferase assays were performed essentially as described⁴⁷. Briefly, 5 μ g of DNA was mixed with DEAE-dextran (50 μ g/ml) in serum-free EBM2, and the resulting mixture was applied onto cells that were 60–80% confluent. 0.125 μ g of pTKRLUC plasmid (Promega, Madison, WI) containing *Renilla* luciferase gene driven by the constitutively active thymidine kinase promoter was used to normalize the transfection efficiencies. After 1 h, cells were exposed to 10% DMSO in serum-free EBM2 for 4 min and then washed twice with PBS and allowed to grow to confluency in EBM2–10% FBS. After appropriate treatments, cells were lysed in passive reporter lysis buffer (Promega) and cell extracts were assayed for firefly and *Renilla* luciferase activities using dual luciferase reporter assay system (Promega). The data were expressed as a ratio of firefly to *Renilla* luciferase activity.

ELISA. Cytokines (IL-6 and IL-1 β) and chemokines (IL-8 and MCP-1) levels in HPAEC culture supernatants were determined using ELISA kits from R&D Systems (Minneapolis, MN) according to the manufacturer's recommendations⁴⁷.

Isolation of cell surface proteins. Cell surface proteins were isolated as per manufacturer's instructions (ab 206998). Confluent EC were rinsed twice with PBS and then covered with ice-cold Sulfo-NHS-SS-Biotin solution. The plates were gently shaken at 4 °C for 30 minutes and the reaction was stopped using quenching solution. Cells were gently scraped and lysed with radioimmune precipitation buffer. To purify surface proteins, the lysate was mixed with Streptavidin beads and incubated at room temperature for 1.5 hours. The bound cell surface proteins were eluted in 100 μ l of elution buffer containing DTT and the proteins in the eluate were then separated on a SDS-PAGE for further analysis.

Immunofluorescence. HPAEC grown to confluence on 2% gelatin-coated coverslips were subjected to immunofluorescence staining as per the protocol described⁵¹. Polyclonal antibody from BD Biosciences was used to visualize VE-cadherin. Nuclei were visualized using DAPI. Following staining the coverslips were rinsed in PBS and mounted on the slide using Vectashield mounting media (Vector Laboratories, Lincolnshire, IL). Images were obtained using a Nikon fluorescence microscope (Nikon Instech, Tokyo, Japan).

In vitro measurement of endothelial permeability by transendothelial electrical resistance (TER). Electrical cell-substrate impedance sensing (ECIS) system from Applied Biophysics, Troy, NY was used to monitor TER, a measure of endothelial barrier integrity, across confluent EC monolayer as described¹³. Briefly, HPAEC were grown to confluence on 2% gelatin coated gold microelectrodes in EBM2 containing 10% FBS and bullet kit additives. 24 h later the complete culture medium was replaced with EBM2 containing 1% FBS. After 2 h the cells were treated as per the experimental requirement followed by thrombin treatment. The TER was monitored for 4–6 h and was normalized to the initial voltage and expressed as a fraction of the normalized resistance value⁴⁷.

Cytosolic Ca²⁺ measurements in intact cell population. HPAEC grown to confluence on 25 mm glass coverslips (Fisher Scientific) were loaded with 2 μ M Fura-2 AM (Invitrogen), a cell permeable fluorescent probe used for measuring change in cytosolic Ca²⁺, for 30 minutes. After dye loading, the cells were washed twice with Ca²⁺ free HBSS buffer, and the coverslips were mounted on an inverted microscope (Eclipse TE2000-E, Nikon). Calcium release from the intracellular stores was determined by perfusing Ca²⁺ free imaging buffer and stimulating cells with thrombin (2.5U). Store-operated Ca²⁺ entry was measured, following addition of 1.26 mM Ca²⁺. Images were captured at 510 nm using a digital CCD camera (CoolSNAP HQ2, Photometrics) and an imaging software (NIS-Element AR 3.0, Nikon) after alternating excitations at 340 and 380 nm. Fura-2 ratio (F-ratio 340/380) was calculated and analyzed later offline with NIS-Element AR 3.0 Software.

Cell adhesion assay. HPAEC grown to confluence in a 96 well black polystyrene plates (Corning), were subjected to adhesion assay as described³⁵. HL-60 cells were labelled with 2.5 μ M Calcein-AM (Invitrogen) for 30 minutes. 200 μ l of Calcein-AM loaded HL-60 cells were added to each well and incubated for 1 hour at 37 °C. After 1 hour the non-adherent cells were removed by gentle wash with Phenol Red free DMEM media. Fluorescence was measured using a fluorescent plate reader at an excitation of 495 nm as described³⁵.

Statistical analysis. Standard one-way ANOVA was used to analyze the results, which were presented as mean \pm SE. Tukey's test (Prism 5.0, GraphPad Software, San Diego) was used to determine the significance between the groups. A *P* value < 0.05 between two groups was considered statistically significant⁴⁷.

References

- Gross, C. M. *et al.* LPS-induced Acute Lung Injury Involves NF-kappaB-mediated Downregulation of SOX18. *Am J Respir Cell Mol Biol* **58**, 614–624, <https://doi.org/10.1165/rcmb.2016-0390OC> (2018).
- Perl, M., Lomas-Neira, J., Venet, E., Chung, C. S. & Ayala, A. Pathogenesis of indirect (secondary) acute lung injury. *Expert review of respiratory medicine* **5**, 115–126, <https://doi.org/10.1586/ers.10.92> (2011).
- Maniatis, N. A., Kotanidou, A., Catravas, J. D. & Orfanos, S. E. Endothelial pathomechanisms in acute lung injury. *Vascul Pharmacol* **49**, 119–133, <https://doi.org/10.1016/j.vph.2008.06.009> (2008).
- Maniatis, N. A. & Orfanos, S. E. The endothelium in acute lung injury/acute respiratory distress syndrome. *Current opinion in critical care* **14**, 22–30, <https://doi.org/10.1097/MCC.0b013e3282f269b9> (2008).
- Minami, T. & Aird, W. C. Endothelial cell gene regulation. *Trends in cardiovascular medicine* **15**, 174–184, doi:10.1050-1738(05)00083-6 [pii] 10.1016/j.tcm.2005.06.002 (2005).
- Rahman, A. & Fazal, F. Hug tightly and say goodbye: role of endothelial ICAM-1 in leukocyte transmigration. *Antioxid Redox Signal* **11**, 823–839, <https://doi.org/10.1089/ARS.2008.2204> (2009).
- Rahman, A. & Fazal, F. Blocking NF-kappaB: an inflammatory issue. *Proceedings of the American Thoracic Society* **8**, 497–503, <https://doi.org/10.1513/pats.201101-009MW> (2011).
- Ye, X., Ding, J., Zhou, X., Chen, G. & Liu, S. F. Divergent roles of endothelial NF-kappaB in multiple organ injury and bacterial clearance in mouse models of sepsis. *The Journal of experimental medicine* **205**, 1303–1315, <https://doi.org/10.1084/jem.20071393> (2008).
- Springer, T. A. Traffic signals for lymphocyte recirculation and leukocyte emigration: the multistep paradigm. *Cell* **76**, 301–314 (1994).
- Bonizzi, G. & Karin, M. The two NF-kappaB activation pathways and their role in innate and adaptive immunity. *Trends Immunol* **25**, 280–288 (2004).
- Birukova, A. A. *et al.* Prostacyclin post-treatment improves LPS-induced acute lung injury and endothelial barrier recovery via Rap1. *Biochim Biophys Acta* **1852**, 778–791, <https://doi.org/10.1016/j.bbadis.2014.12.016> (2015).
- Dudek, S. M. & Garcia, J. G. Cytoskeletal regulation of pulmonary vascular permeability. *J Appl Physiol* **91**, 1487–1500 (2001).
- Mehta, D., Rahman, A. & Malik, A. B. Protein kinase C-alpha signals rho-guanine nucleotide dissociation inhibitor phosphorylation and rho activation and regulates the endothelial cell barrier function. *J Biol Chem* **276**, 22614–22620 (2001).
- Tirupathi, C., Ahmmed, G. U., Vogel, S. M. & Malik, A. B. Ca²⁺ signaling, TRP channels, and endothelial permeability. *Microcirculation* **13**, 693–708, <https://doi.org/10.1080/10739680600930347> (2006).
- Lucas, R., Verin, A. D., Black, S. M. & Catravas, J. D. Regulators of endothelial and epithelial barrier integrity and function in acute lung injury. *Biochemical pharmacology* **77**, 1763–1772, <https://doi.org/10.1016/j.bcp.2009.01.014> (2009).
- Bhattacharya, J. & Matthay, M. A. Regulation and repair of the alveolar-capillary barrier in acute lung injury. *Annual review of physiology* **75**, 593–615, <https://doi.org/10.1146/annurev-physiol-030212-183756> (2013).
- Bijli, K. M. *et al.* Regulation of endothelial cell inflammation and lung polymorphonuclear lymphocyte infiltration by transglutaminase 2. *Shock* **42**, 562–569, <https://doi.org/10.1097/SHK.0000000000000242> (2014).
- Fazal, F. *et al.* Critical role of non-muscle myosin light chain kinase in thrombin-induced endothelial cell inflammation and lung PMN infiltration. *PLoS one* **8**, e59965, <https://doi.org/10.1371/journal.pone.0059965> (2013).
- Gong, H. *et al.* HIF2alpha signaling inhibits adherens junctional disruption in acute lung injury. *The Journal of clinical investigation* **125**, 652–664, <https://doi.org/10.1172/JCI177701> (2015).
- Ware, L. B. & Matthay, M. A. The acute respiratory distress syndrome. *The New England journal of medicine* **342**, 1334–1349, <https://doi.org/10.1056/NEJM200005043421806> (2000).
- Xu, C., Bailly-Maitre, B. & Reed, J. C. Endoplasmic reticulum stress: cell life and death decisions. *The Journal of clinical investigation* **115**, 2656–2664, <https://doi.org/10.1172/JCI26373> (2005).
- Leonard, A., Paton, A. W., El-Quadi, M., Paton, J. C. & Fazal, F. Preconditioning with endoplasmic reticulum stress ameliorates endothelial cell inflammation. *PLoS one* **9**, e110949, <https://doi.org/10.1371/journal.pone.0110949> (2014).
- Ni, M., Zhang, Y. & Lee, A. S. Beyond the endoplasmic reticulum: atypical GRP78 in cell viability, signalling and therapeutic targeting. *The Biochemical journal* **434**, 181–188, <https://doi.org/10.1042/BJ20101569> (2011).
- Kim, I., Xu, W. & Reed, J. C. Cell death and endoplasmic reticulum stress: disease relevance and therapeutic opportunities. *Nature reviews. Drug discovery* **7**, 1013–1030, <https://doi.org/10.1038/nrd2755> (2008).
- Hotamisligil, G. S. Endoplasmic reticulum stress and the inflammatory basis of metabolic disease. *Cell* **140**, 900–917, <https://doi.org/10.1016/j.cell.2010.02.034> (2010).
- Hotamisligil, G. S. Endoplasmic reticulum stress and atherosclerosis. *Nature medicine* **16**, 396–399, <https://doi.org/10.1038/nm0410-396> (2010).
- Garg, A. D. *et al.* ER stress-induced inflammation: does it aid or impede disease progression? *Trends in molecular medicine* **18**, 589–598, <https://doi.org/10.1016/j.molmed.2012.06.010> (2012).
- Paton, A. W. *et al.* AB5 subtilase cytotoxin inactivates the endoplasmic reticulum chaperone BiP. *Nature* **443**, 548–552, <https://doi.org/10.1038/nature05124> (2006).
- Ray, R. *et al.* The Escherichia coli subtilase cytotoxin A subunit specifically cleaves cell-surface GRP78 protein and abolishes COOH-terminal-dependent signaling. *J Biol Chem* **287**, 32755–32769, <https://doi.org/10.1074/jbc.M112.399808> (2012).
- McLean, J. W. *et al.* Organ-specific endothelial cell uptake of cationic liposome-DNA complexes in mice. *Am J Physiol* **273**, H387–404 (1997).
- Thurston, G. *et al.* Cationic liposomes target angiogenic endothelial cells in tumors and chronic inflammation in mice. *The Journal of clinical investigation* **101**, 1401–1413 (1998).
- Xu, N., Rahman, A., Minshall, R. D., Tirupathi, C. & Malik, A. B. beta(2)-Integrin blockade driven by E-selectin promoter prevents neutrophil sequestration and lung injury in mice. *Circ Res* **87**, 254–260 (2000).
- Carlisle, R. E. *et al.* 4-Phenylbutyrate inhibits tunicamycin-induced acute kidney injury via CHOP/GADD153 repression. *PLoS one* **9**, e84663, <https://doi.org/10.1371/journal.pone.0084663> (2014).
- Dvorin, E. L., Jacobson, J., Roth, S. J. & Bischoff, J. Human pulmonary valve endothelial cells express functional adhesion molecules for leukocytes. *The Journal of heart valve disease* **12**, 617–624 (2003).
- Leonard, A., Rahman, A. & Fazal, F. Importins alpha and beta signaling mediates endothelial cell inflammation and barrier disruption. *Cellular signalling* **44**, 103–117, <https://doi.org/10.1016/j.cellsig.2018.01.011> (2018).
- Nilius, B. & Droogmans, G. Ion channels and their functional role in vascular endothelium. *Physiol Rev* **81**, 1415–1459, <https://doi.org/10.1152/physrev.2001.81.4.1415> (2001).
- Birukova, A. A. *et al.* GRP78 is a novel receptor initiating a vascular barrier protective response to oxidized phospholipids. *Mol Biol Cell* **25**, 2006–2016, <https://doi.org/10.1091/mbc.E13-12-0743> (2014).

38. Philippova, M. *et al.* Identification of proteins associating with glycosylphosphatidylinositol- anchored T-cadherin on the surface of vascular endothelial cells: role for Grp78/BiP in T-cadherin-dependent cell survival. *Mol Cell Biol* **28**, 4004–4017, <https://doi.org/10.1128/MCB.00157-08> (2008).
39. Dejana, E. & Vestweber, D. The role of VE-cadherin in vascular morphogenesis and permeability control. *Progress in molecular biology and translational science* **116**, 119–144, <https://doi.org/10.1016/B978-0-12-394311-8.00006-6> (2013).
40. Mehta, D. & Malik, A. B. Signaling mechanisms regulating endothelial permeability. *Physiol Rev* **86**, 279–367, <https://doi.org/10.1152/physrev.00012.2005> (2006).
41. Parekh, A. B. Store-operated CRAC channels: function in health and disease. *Nature reviews. Drug discovery* **9**, 399–410, <https://doi.org/10.1038/nrd3136> (2010).
42. Zhang, S. L. *et al.* STIM1 is a Ca²⁺ sensor that activates CRAC channels and migrates from the Ca²⁺ store to the plasma membrane. *Nature* **437**, 902–905, <https://doi.org/10.1038/nature04147> (2005).
43. Park, C. Y. *et al.* STIM1 clusters and activates CRAC channels via direct binding of a cytosolic domain to Orai1. *Cell* **136**, 876–890, <https://doi.org/10.1016/j.cell.2009.02.014> (2009).
44. Yazbeck, P. *et al.* STIM1 Phosphorylation at Y361 Recruits Orai1 to STIM1 Puncta and Induces Ca(2+) Entry. *Scientific reports* **7**, 42758, <https://doi.org/10.1038/srep42758> (2017).
45. Sundivakkam, P. C., Natarajan, V., Malik, A. B. & Tirupathi, C. Store-operated Ca²⁺ entry (SOCE) induced by protease-activated receptor-1 mediates STIM1 protein phosphorylation to inhibit SOCE in endothelial cells through AMP-activated protein kinase and p38beta mitogen-activated protein kinase. *J Biol Chem* **288**, 17030–17041, <https://doi.org/10.1074/jbc.M112.411272> (2013).
46. Paton, A. W., Srimanote, P., Talbot, U. M., Wang, H. & Paton, J. C. A new family of potent AB(5) cytotoxins produced by Shiga toxicigenic Escherichia coli. *The Journal of experimental medicine* **200**, 35–46, <https://doi.org/10.1084/jem.20040392> (2004).
47. Bijli, K. M. *et al.* Phospholipase C-epsilon signaling mediates endothelial cell inflammation and barrier disruption in acute lung injury. *Am J Physiol Lung Cell Mol Physiol* **311**, L517–524, <https://doi.org/10.1152/ajplung.00069.2016> (2016).
48. Mittal, M. *et al.* TNFalpha-stimulated gene-6 (TSG6) activates macrophage phenotype transition to prevent inflammatory lung injury. *Proc Natl Acad Sci USA* **113**, E8151–E8158, <https://doi.org/10.1073/pnas.1614935113> (2016).
49. Slavin, S. A., Leonard, A., Grose, V., Fazal, F. & Rahman, A. Autophagy inhibitor 3-methyladenine protects against endothelial cell barrier dysfunction in acute lung injury. *Am J Physiol Lung Cell Mol Physiol* **314**, L388–L396, <https://doi.org/10.1152/ajplung.00555.2016> (2018).
50. Bello-Irizarry, S. N., Wang, J., Johnston, C. J., Gigliotti, F. & Wright, T. W. MyD88 signaling regulates both host defense and immunopathogenesis during pneumocystis infection. *J Immunol* **192**, 282–292, <https://doi.org/10.4049/jimmunol.1301431> (2014).
51. Fazal, F., Minhajuddin, M., Bijli, K. M., McGrath, J. L. & Rahman, A. Evidence for actin cytoskeleton-dependent and -independent pathways for RelA/p65 nuclear translocation in endothelial cells. *J Biol Chem* **282**, 3940–3950 (2007).

Acknowledgements

We would like to thank Jane Malone, Research Scientist in the Department of Pediatrics, for assistance in measuring lung compliance in mice (Fig. 1G). This work was supported by National Heart Lung and Blood Institute grants HL130870, GM130463 and HL116632.

Author Contributions

F.F., A.L. and A.R. conceived and designed the experiments. A.L. and V.G. performed the experiments. F.F. analyzed the data and drafted the manuscript. J.P. and A.P. contributed the reagents for the study. F.F., A.P., J.P., D.Y. and A.R. edited and approved the final version of the manuscript.

Additional Information

Competing Interests: The authors declare no competing interests.

Publisher's note: Springer Nature remains neutral with regard to jurisdictional claims in published maps and institutional affiliations.



Open Access This article is licensed under a Creative Commons Attribution 4.0 International License, which permits use, sharing, adaptation, distribution and reproduction in any medium or format, as long as you give appropriate credit to the original author(s) and the source, provide a link to the Creative Commons license, and indicate if changes were made. The images or other third party material in this article are included in the article's Creative Commons license, unless indicated otherwise in a credit line to the material. If material is not included in the article's Creative Commons license and your intended use is not permitted by statutory regulation or exceeds the permitted use, you will need to obtain permission directly from the copyright holder. To view a copy of this license, visit <http://creativecommons.org/licenses/by/4.0/>.

© The Author(s) 2019